INS/GNSS/Odometer Data Fusion in Railway Applications

Symposium

Inertial Sensors & Systems

Karlsruhe / Germany, 09/2016

C. Reimer, E. L. v. Hinüber

iMAR Navigation GmbH
Im Reihersbruch 3
66386 St. Ingbert
GERMANY

Inertial Sensors and Systems 2016

Karlsruhe, Germany

Abstract

Integrated navigation systems installed on trains usually make use of data fusion of GNSS data, INS data and wheel velocity data. Since the connection between the carriage body of the wagon and the wheel is not rigid, special considerations need to be taken into account to achieve a mostly optimal behavior of the integrated navigation solution even under prolonged GNSS outages.

In this paper, an approach to deal with this problem is presented and its effectiveness is evaluated with experimental test data from the brand new 57 km Gotthard Base Tunnel (GBT) in Switzerland.

Using a navigation-grade RLG based INS of type iNAT-RQT-4003, errors < 15 m for a complete passage are achieved with the presented approach.

1. Introduction

Data fusion of inertial navigation systems with outputs from both GNSS (global positioning systems like GPS or GLONASS) on the one hand and wheel velocity measurement systems (like wheel mounted encoder or radar based systems) on the other hand is a well-studied problem and extensive research has been conducted on optimal data fusion techniques for this scenario [1][2][3]. Both of these systems are readily available on land vehicles and represent attractive aiding sources to attenuate inertial drift errors because of their ease of use and comparatively low costs. While the integration of a 6-axis IMU allows a very accurate propagation model of the navigation solution, vehicle motion models may still be used as pseudo-measurement inputs to the integration filter [2]. Common examples for such so-called non-holonomic constraint aidings for land vehicles are zero lateral velocity updates or (if lower grade gyros are being used) zero heading rate updates while the vehicle is stationary. Section 2 gives a brief overview of the integration Kalman filter architecture used in this paper.

When using zero-lateral velocity aiding, mounting misalignments between the INS and the vehicle have to be accurately known or have to be estimated in the integration filter. The fundamental assumption for this estimation is usually that the main travelling axis is fixed in both the vehicle coordinate frame and the INS coordinate frame. While this is a valid assumption in e.g. automotive applications for the misalignment between the car body and the rear axis, it does not hold true for railway applications, where the carriage box is usually separated from the rail-wheel system by a flexible structure which is called the bogie.

Thus, special considerations have to be taken into account to compensate for this misalignment between the carriage box containing the INS and the wheel system. Section 3 of this paper deals with this problem.

Finally, results obtained from a measurement campaign in the 57 km long, newly opened Gotthard Base Tunnel are presented in Section 4 to evaluate the effectiveness of the presented data fusion approach.

2. System Model

2.1 Navigation Differential Equations

The INS uses initial values for the navigation parameters and the output of its accelerometers and gyroscopes to integrate the navigation equations in an earth-centered and earth-fixed (ECEF) frame.

$$\dot{\vec{r}}^e = \vec{v}^e_{eb} \tag{1}$$

$$\dot{\vec{v}}^e_{eb} = C^e_b \vec{f}^b_{ib} - 2\vec{\omega}^e_{ie} \times \vec{v}^e_{eb} + \vec{g}^e(\vec{r}^e) \tag{2}$$

$$\dot{C}^e_b = C^e_b \Omega^b_{ib} - \Omega^e_{ie} C^e_b \tag{3}$$

where

$\vec{f}^b_{ib}$ is the specific force measured by the accelerometers,

$\vec{\omega}^b_{ib}$= the angular rate measured by the gyroscopes

$\Omega = [\vec{\omega} \times] = \begin{pmatrix} 0 & -\omega_z & \omega_y \\ \omega_z & 0 & -\omega_x \\ -\omega_y & \omega_x & 0 \end{pmatrix}$ is a skew symmetric matrix representing a cross-product

C^e_b is the transformation matrix from the current b-frame (body) to the current ECEF-frame

$\vec{r}^e$ is the current position of the INS with respect to earth in the ECEF frame

$\vec{\omega}^e_{ie} = (0 \quad 0 \quad \omega_e)^T$ is the earth rotation rate

$\vec{g}^e(\vec{r}^e)$ is the value of gravity at the current INS position

$\vec{v}^e_{eb}$ is the current velocity of the INS with respect to earth in the ECEF frame

The ECEF frame axes are defined to originate from the earth center, the z axis pointing to the north pole and the x axis pointing to the intersection point of the prime meridian and the equator. The y axis completes the right-hand coordinate system.

2.2 Navigation Error Differential Equations

Due to initialization, instrument and gravity model errors, the INS accumulates errors over time, which is commonly termed as drift. Since the dynamics of the errors of the computed navigation parameters are usually much lower than the dynamics of the navigation parameters themselves, it is advantageous to formulate the Kalman filter to track only the errors of the INS [2]. Assuming only small attitude errors, neglecting second order error effects and following the derivation in e.g. [2], the following INS error differential equations are obtained:

$$\delta\dot{\vec{r}}^{e} = \frac{d}{dt}(\hat{\vec{r}}^{e} - \vec{r}^{e}) = \delta\vec{v}_{eb}^{e} \tag{4}$$

$$\delta\dot{\vec{v}}_{eb}^{e} = \frac{d}{dt}\left(\hat{\vec{v}}_{eb}^{e} - \vec{v}_{eb}^{e}\right) = \left[\vec{f}_{ib}^{e}\times\right]\vec{\psi}^{e} + C_{b}^{e}\delta\vec{f}_{ib}^{b} - 2\vec{\omega}_{ie}^{e}\times\delta\vec{v}_{eb}^{e} + \vec{g}_{m}^{e}\left(\hat{\vec{r}}^{e}\right) - \vec{g}_{m}^{e}(\vec{r}^{e}) - \delta\vec{g}_{m}^{e}(\vec{r}^{e}) \tag{5}$$

$$\dot{\vec{\psi}}^{e} = \hat{C}_{b}^{e}\delta\vec{\omega}_{ib}^{b} - \vec{\omega}_{ie}^{e}\times\vec{\psi}^{e} \tag{6}$$

where

$\hat{x}$ is an estimated or computed value x

δx is the difference between the estimated and the true value of x, i.e. $\hat{x} = x + \delta x$

$\vec{g}_{m}^{e}(x)$ is the gravity predicted by the gravity model at x

$\delta\vec{g}_{m}^{e}(\vec{r}^{e})$ is the error in the gravity model at the true INS location

and $\vec{\psi}^{e}$ defines the small angle error model by

$$C_{b}^{e} = (I_{3\times3} + \Psi^{e})\hat{C}_{b}^{e} \tag{7}$$

2.3 Error State Space Kalman Filter

These equations form the basis for the propagation phase of the error state space Kalman filter used for fusing the INS solution with GNSS and wheel velocity measurements. The Kalman filter uses navigation parameter errors augmented by instrument and aiding sensor errors as its state vector $\vec{x}_{EKF}$:

$$\vec{x}_{EKF} = \left(\delta\vec{r}^{e}, \delta\vec{v}_{eb}^{e}, \vec{\psi}^{e}, \vec{b}_{a}, \vec{b}_{g}, \delta\vec{C}_{a}, \delta\vec{C}_{g}, \delta\vec{x}_{GNSS}, \delta\vec{x}_{Odo}\right) \tag{8}$$

Depending on which sensor errors are dominant or observable, certain parts of the instrument error vector may be omitted for certain sensor types or applications.

The GNSS part of the state vector comprises clock offsets and drift, where the drift is the time derivative of the offset.

The odometer part of the state vector comprises an odometer scale factor error δs_{Odo} and two small misalignment angles $\vec{\psi}^v = (0 \quad \psi_{v,y} \quad \psi_{v,z})^T$ between nominal and actual vehicle axes.

2.3.1. Propagation Step

During the propagation step of the Kalman filter, the state covariance matrix is updated by the following equations:

$$P_k^- = \Phi_{k,k-1} P_{k-1}^+ \Phi_{k,k-1}^T + Q_k \tag{9}$$

In this equation, $\Phi_{k,k-1}$ represents the matrix exponential of the Jacobian A of the system differential equations times the update interval ΔT, which is approximated using the first two terms of the Taylor expansion:

$$\Phi_{k,k-1} \approx I + A\Delta T + \frac{1}{2} A^2 \Delta T^2 \tag{10}$$

Q_k represents the process noise matrix whose contents mainly depend on the quality of the inertial sensors which are used as well as environmental conditions like vibration levels or temperature gradients.

Since the Kalman filter is operating in a closed loop mode and odometer errors comprise random constants, the state propagation can be omitted for the navigation parameter, instrument and odometer errors and only needs to be implemented for the additional GNSS states.

2.3.2 Measurement Step

2.3.2.1. GNSS Measurements

The difference between the predicted ranges and the pseudoranges measured by the GNSS receiver are used as a measurement in the Kalman filter. The predicted range to the k-th satellite can be expressed as:

$$\hat{\rho}_k = \vec{e}_k^T (\vec{r}_{s,k}^e - \hat{\vec{r}}_a^e) \tag{11}$$

where

$\vec{e}_k$ is a unit vector pointing from the GNSS antenna to the k-th satellite,

$\vec{r}_{s,k}^e$ is the position of the k-th satellite at the time of signal transmission in the ECEF frame at the time of signal reception and

$\vec{r}_a^e$ is the position of vehicle GNSS antenna at the time of signal reception in the ECEF frame.

Similarly, the measured pseudoranges may be expressed as (neglecting satellite-specific range biases)

$$\rho_k = \vec{e}_k^T\left(\vec{r}_{s,k}^e - \vec{r}_a^e\right) + c\Delta T + n_k \tag{12}$$

where

$c\Delta T$ is the GNSS receiver clock error times speed of light and

n_k is the GNSS receiver pseudorange random noise.

Taking the difference of the above equations, one obtains

$$\hat{\rho}_k - \rho_k = -\vec{e}_k^T\left(\hat{\vec{r}}_a^e - \vec{r}_a^e\right) - c\Delta T + \tilde{n}_k \tag{13}$$

The difference between the predicted antenna position and the actual antenna position may be further resolved as

$$\hat{\vec{r}}_a^e - \vec{r}_a^e = \delta\vec{r}^e - \left[\left(\hat{C}_b^e\vec{l}_{ba}^b\right)\times\right]\vec{\psi}^e \tag{14}$$

This yields the measurement prediction function $h_{GNSS}(\vec{x}_{EKF})$ as

$$h_{GNSS}(\vec{x}_{EKF}) = -\vec{e}_k^T\left(\delta\vec{r}^e - \left[\left(\hat{C}_b^e\vec{l}_{ba}^b\right)\times\right]\vec{\psi}^e\right) - c\Delta T \tag{15}$$

and the measurement matrix H is given by

$$H = \left(-\vec{e}_k^T \mid 0_{1\times3}\mid - \vec{e}_k^T\left[\hat{l}_{ba}^e\times\right] \mid 0_{1\times21}\mid -1\mid 0_{1\times4}\right) \tag{16}$$

2.3.2.2. Wheel Velocity Measurements

For odometer aiding in combination with zero lateral velocity updates, the difference between the predicted velocity in the forward/backward direction and two axes perpendicular to this and a vector comprising the measured wheel speed and zeros for the lateral directions is used as an input to the Kalman filter. In terms of INS state estimate, INS errors and odometer errors, this measurement may be expressed as:

$$\vec{y} = \hat{C}_b^v\left(\hat{C}_e^b\hat{\vec{v}}_{eb}^e + \vec{\omega}_{ib}^b\times\vec{l}_{odo}^b\right) - M_s(I_{3\times3} + \Psi^v)\hat{C}_b^v(\hat{C}_e^b(I_{3\times3} - \Psi^e)\left(\hat{\vec{v}}_{eb}^e - \delta\vec{v}_{eb}^e\right) + \vec{\omega}_{ib}^b\times\vec{l}_{odo}^b) \tag{17}$$

where

$\hat{C}_b^v$ is the transformation matrix representing the nominal misalignment between INS body frame and vehicle frame,

$\vec{l}_{odo}^{\,b}$ is the lever arm to the odometer in INS body frame and

$M_s = \begin{pmatrix} 1+\delta s_{odo} & 0 & 0 \\ 0 & 1 & 0 \\ 0 & 0 & 1 \end{pmatrix}$ is the odometer scale factor error matrix.

Errors in the measured angular rate are neglected since these are well below contributions of noise and other un-modeled errors on this measurement. Equation (17) may be used to derive the measurement matrix H using a CAS (omitted here for brevity).

3. Railway Application Specifics

The INS is usually located inside a carriage box on the train. The carriage box is mounted on the bogie, which is carrying the wheels, through a bogie pin and several springs and dampers. Figure 1 shows a typical bogie assembly. This structure allows for a certain degree of rotation between the carriage box and the wheels, which allows to pass smaller curve radii and it improves the ride quality for passengers.

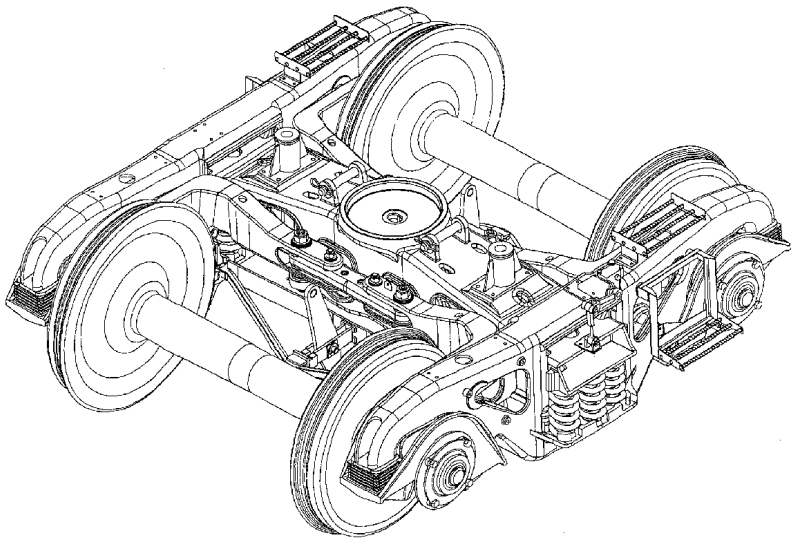

Figure 1: Bogie, containing four train wheels (Source: http://www.drehgestelle.de/6/Scheffel_LKAB2.gif)

This assembly, however, creates a problem for the use of zero lateral velocity updates: In curves, the carriage box will lie on the secant between the two bogie pins, and the bogies will approximately be tangential to the curve, creating a misalignment between the odometer frame, in which the zero lateral velocity assumption is still valid, and the vehicle

frame, where it is now violated. Denoting the distance between the two bogie pins of the carriage box as *d* and the current curve radius as *R*, the misalignment between secant and tangent and thus between bogie and carriage box is given by:

$$\alpha = \sin^{-1}\frac{d}{2R} \tag{18}$$

The misalignment between train and bogie for different curve radii (assuming a bogie to bogie distance of 19 m) is depicted in Figure 2.

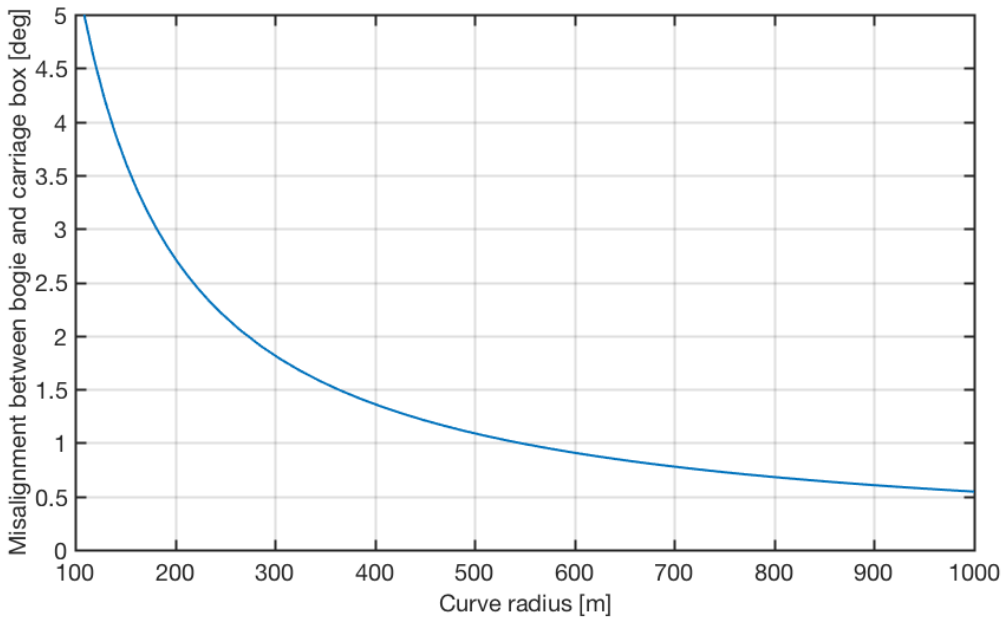

Figure 2: Misalignment between bogie and carriage box for different curve radii

The following figure shows the relations between bogie and carrier box.

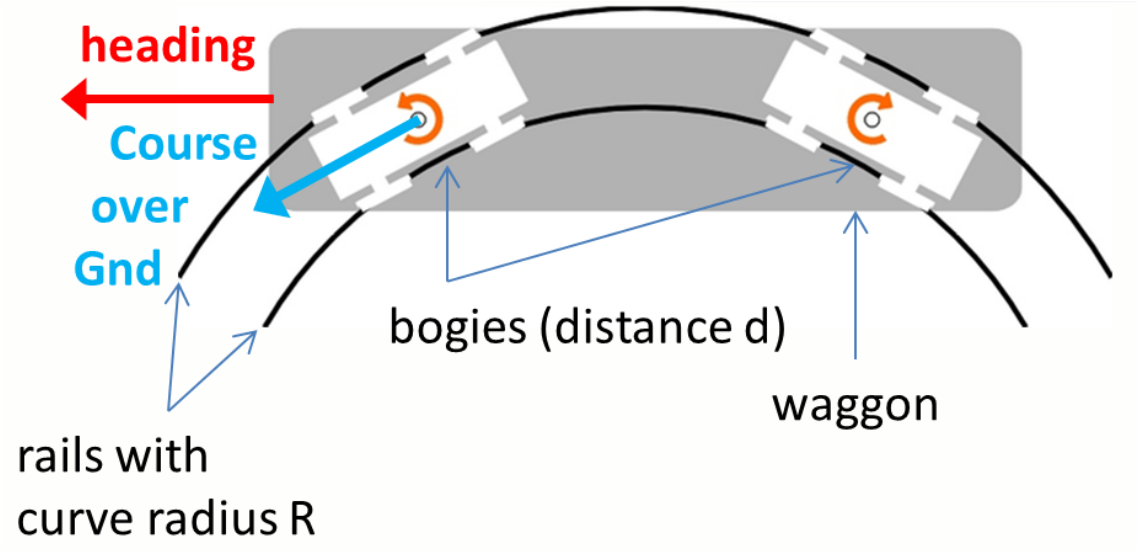

Figure 3: Relation between bogie, carriage, heading and course over ground

To assess how much of a problem this is for the zero lateral velocity updates, we assume a velocity of 270 km/h (75 m/s), a distance of 19 m between the bogie pins and a curve radius of 5000 m (i.e. the values of an ICE train travelling through the Gotthard Base Tunnel). The velocity error due to the misalignment will be

$$\Delta v_{lat} = \frac{d}{2R} v_{lon} = 0.14\ m/s \tag{19}$$

This means that when driving with the maximum speed of 75 m/s through the curve, the zero lateral velocity measurement innovation will be biased by 0.14 m/s if this error is left uncompensated. This would pose a large risk to corrupt the EKF state estimates.

To compensate for this misalignment, it has to be measured by e.g. optical devices or the curve radius has to be known. Since optical measurement of the misalignment between bogie and pin requires specialized equipment and modifications to the bogie assembly, it usually is not available. On the other hand, the curve radius may be estimated using the longitudinal velocity and vertical turn rate of the INS:

$$v_{lon} = \omega_d R \Leftrightarrow R = \frac{v_{lon}}{\omega_d} \tag{20}$$

Equations (18) and (20) can now be used to introduce another misalignment matrix into the wheel speed measurement model of (17) to take the bogie to carriage box misalignment into account:

$$\vec{y} = C_\alpha \hat{C}_b^v \left(\hat{C}_e^b \hat{\vec{v}}_{eb}^e + \vec{\omega}_{ib}^b \times \vec{l}_{odo}^b\right) - M_s C_\alpha (I_{3\times3} + \Psi^v) \hat{C}_b^v \left(\hat{C}_e^b (I_{3\times3} - \Psi^e)\left(\hat{\vec{v}}_{eb}^e - \delta\vec{v}_{eb}^e\right) + \vec{\omega}_{ib}^b \times \vec{l}_{odo}^b\right) \tag{21}$$

where

$C_\alpha = \begin{pmatrix} \cos\alpha & \sin\alpha & 0 \\ -\sin\alpha & \cos\alpha & 0 \\ 0 & 0 & 1 \end{pmatrix}$ is the misalignment matrix correcting for the misalignment between carriage box and the bogie carrying the measured wheel.

Equation (21) again may be used to derive the measurement matrix H using a CAS (omitted here for brevity).

4. Test Results

4.1. Test Description

After performing unsuccessful measurements over about two years with an inertial navigation system being provided by a competing system manufacturer, Swiss Federal Railways (Schweizerische Bundesbahn, SBB) acquired from iMAR Navigation in October 2015 an

INS of type iNAT-RQT-4003 following successful tests in September 2015. It is used in an RF (radio frequency) measurement train for geo-referencing RF measurement results. Background is, that the prove of sufficient RF communication availablility on each position inside the tunnel is the prerequisite to approve the safety concept of the entire GBT. One possible way to geo-reference this data would be to use track kilometrage. The downside of this is that kilometrage is subject to change over the years as modifications alter the railway network. These changes then usually need some weeks to several months to propagate into central databases relating kilometrage to geodetic coordinates. Using the INS navigation result instead of kilometrage for geo-referencing allows SBB very quick assessment of possible problematic areas and as a consequence a quick turnaround time to fix problems and validating RF performance after these fixes.

The compensation of the misalignment between carriage box and bogie could be tested during surveys of the recently opened Gotthard Base Tunnel on this RF detector train as well as on a rented ICE measurement train (from Deutsche Bahn) for the high-speed tests.

The Gotthard Base Tunnel has a total length of around 57 km. To acquire the license to operate the tunnel with maximum train speeds of 250 km/h, acceptance tests for the RF signaling equipment had to be conducted for speeds of up to 275 km/h. In the following, some results obtained during these high-speed tests are presented.

4.2 Test Setup

Figure 4: iMAR iNAT-RQT-4003 (INS/GNSS system with odometer interface)

The iNAT-RQT-4003 (Figure 4, specification in Table 1) was installed on the bottom of the carriage box of the train with its x-axis pointing into the longitudinal direction of the train and its z-Axis pointing down.

Table 1: IMU specification of iNAT-RQT-4003

	Accelerometers	**Gyroscopes**
Day-to-day bias	< 100 µg	< 0.01 deg/h
Random walk	< 12 µg/sqrt(Hz)	< 0.005 deg/sqrt(h)
Bias stability (AVAR)	< 12 µg	< 0.0015 deg/h
Range	20 g	+/- 395 deg/s
Scale factor error	< 100 ppm	< 15 ppm

The integrated geodetic GNSS receiver was connected to a rail vehicle certified L1 antenna located on the roof of the train and the antenna offset was entered with an estimated error of less than 10 cm. The odometer lever arm was entered as the lever arm to the bogie pin of the bogie containing the measured wheel. The rationale behind this is that due to conic profile of the train wheels (see Figure 5) the wheel speed varies e.g. in curves, but since the wheel is connected to the opposing wheel by a rigid axis, the average wheel speed will be that of the axis middle point. Similarly, since the distance between the two axes of the bogie is fixed, this average speed will be the same speed that would be measured in the center between them, i.e. at the bogie pin. The bogie pin to bogie pin distance between the two bogies was configured according to the datasheet of the train.

Figure 5: Typical conical train wheel profile (Source: http://www.etudes.ru/data/etudes/wagonwheels/17.jpg)

iNAT-RQT-4003 supports a coarse scale factor calibration which sets up the sign and a rough magnitude of the odometer scale factor during the first few hundred meters of travel after initial alignment, allowing for a very easy setup. The complete real-time navigation result as well as raw GNSS, wheel velocity and inertial data were recorded to the internal storage of the iNAT-RQT-4003, which has enough capacity for several days of measurement data. This recorded data can be retrieved from the device via FTP access, e.g. using iMAR's iXCOM-CMD software, which is also used to configure the system and to visualize measuring data in real-time or in post-mission. The customer electronics received the real-time INS solution via NMEA183 over an UART RS422 interface as well as via Ethernet, using the iXCOM protocol interface.

4.3 Test Results

Figure 6 depicts the overall trajectory of the test. Totally, 8 passages through the tunnel were recorded. The total accumulated position error for each passage as well as separate along-track and cross-track components are given in Table 2.

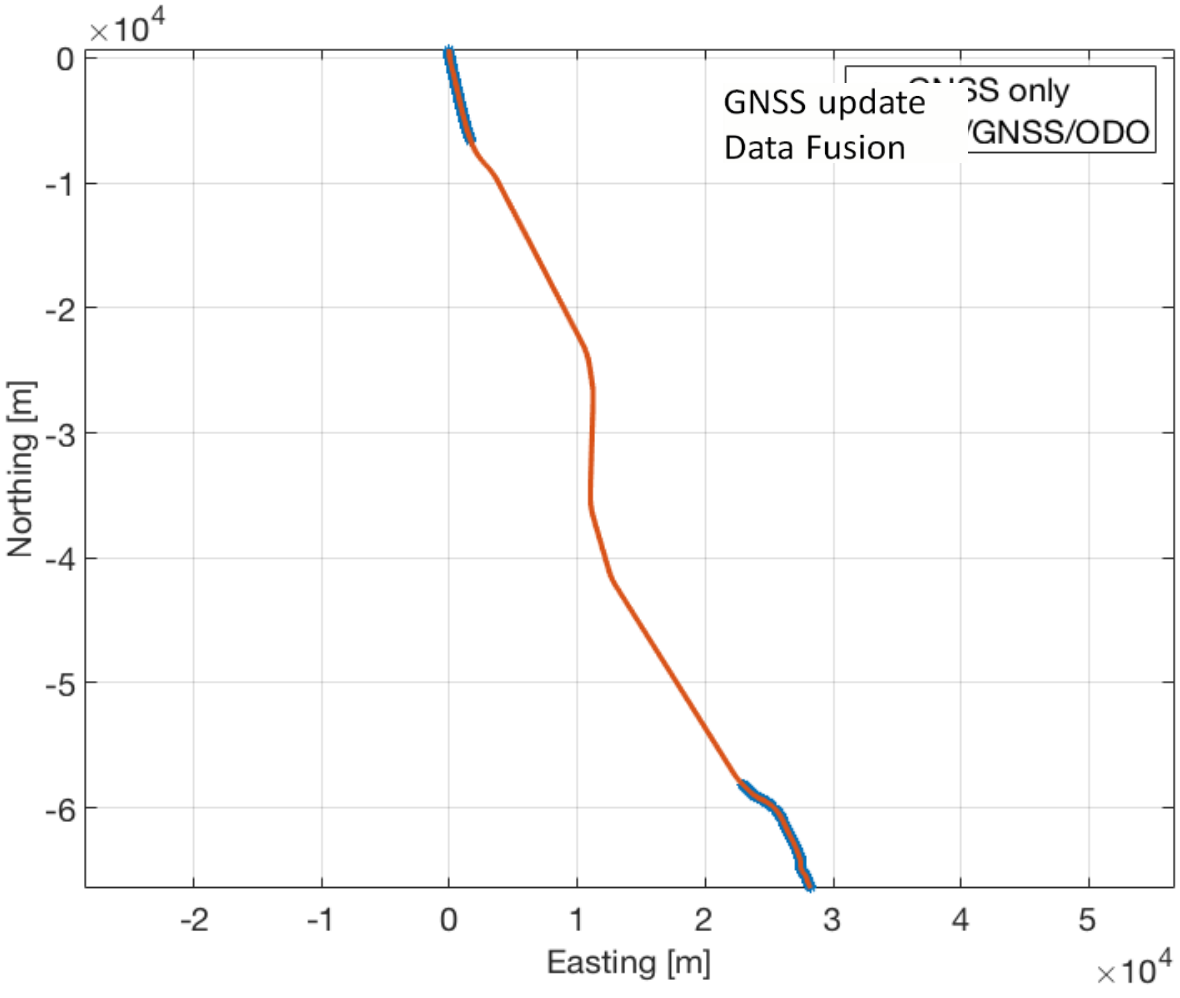

Figure 6: Gotthard Base Tunnel trajectory

When comparing this with classical dead-reckoning navigation, the maximum along-track error corresponds to a scale error of only 0.04 %, while the cross track-error corresponds to a maximum heading error of only 0.24 mrad, validating the performance of the proposed data fusion approach.

Table 2: Position correction impulses after passages

Passage No.	Total error	Along track error	Cross track error
1	16.16 m	3.91 m	15.68 m
2	27.29 m	25.34 m	10.13 m
3	11.12 m	9.05 m	6.46 m
4	15.67 m	15.61 m	1.46 m
5	6.37 m	2.42 m	5.89 m
6	11.97 m	11.73 m	2.40 m
7	13.97 m	2.67 m	13.71 m
8	19.2 m	16.93 m	9.07 m

To validate the performance of the misalignment compensation described in section 3, the INS velocity has been transformed to the location of the bogie pin and was compared to the vehicle heading (including the estimated misalignment between INS and vehicle). The result of a single passage through the tunnel is depicted in Figure 7.

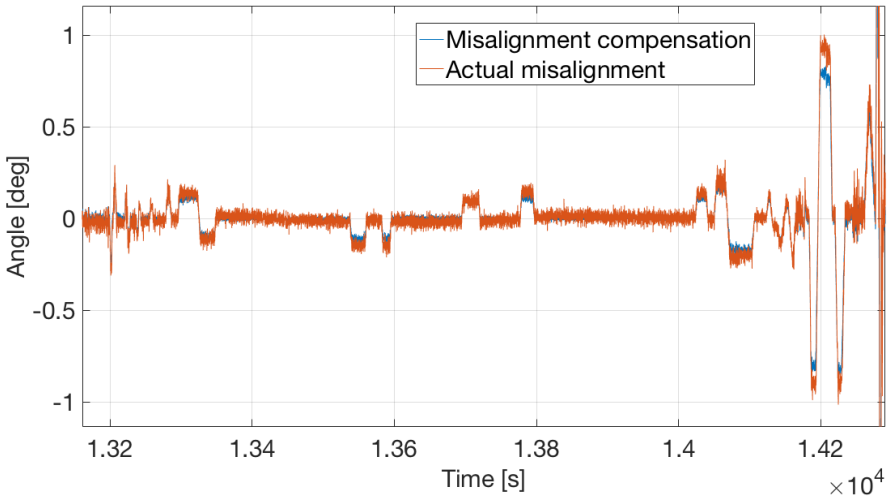

Figure 7: Misalignment compensation vs. actual misalignment

The minimum curve radius of the tunnel is 5000 m, corresponding to a maximum misalignment of about 0.21 deg inside of the tunnel. For these small angles, the misalignment compensation performs very well, while for smaller curve radii (e.g. approx. 1000 m for a misalignment of 1 deg), there seems to be a modeling error leading to underestimation of the misalignment angle. The reason for this is that these smaller curve radii correspond to crossovers which may not be modeled as circular segments (clothoid).

5. Conclusion and Outlook

The effectiveness of the data fusion strategy has been demonstrated using the test data obtained from several passages through the 57 km long Gotthard Base Tunnel. The proposed compensation scheme for the misalignment between carriage box and bogie has been demonstrated to agree very well with the actual difference between course over ground and vehicle heading at the bogie pin, as long as the assumption of circular curve segments holds true.

While during these tests an RLG-based INS has been used, the same algorithms are available on iMAR's complete iNAT family, ranging from RLG and hemispheric resonator gyro based navigation grade devices over to FOG and MEMS based tactical and consumer grade devices. Upon request, a test report for the MEMS based iNAT-M200-SLN demonstrating a performance of lateral errors of only 25 m after a 600 s lasting GNSS and after travelling 20 km outage can be made available (see also www.imar-navigation.de).

6. Acknowledgements

The authors would like to thank Mr H. Vetsch of SBB for the provision of the recorded data and the permission to publish results obtained from the surveying campaign.

References

[1] Kim, S. B., Bazin, J. C., Lee, H. K., Choi, K. H., & Park, S. Y, "Ground vehicle navigation in harsh urban conditions by integrating inertial navigation system, global positioning system, odometer and vision data", IET radar, sonar & navigation, 2011

[2] P. D. Groves, "GNSS, Inertial and Multisensor Integrated Navigation Systems", Artech House, USA, 2013

[3] J. Wendel, "Integrierte Navigationssysteme. Sensordatenfusion, GPS und Inertiale Navigation", Oldenbourg Verlag, Germany, 2007